

Strong Ligand–Protein Interactions Revealed by Ultrafast Infrared Spectroscopy of CO in the Heme Pocket of the Oxygen Sensor FixL

Patrick Nuernberger,^{†,‡,§} Kevin F. Lee,^{†,‡} Adeline Bonvalet,^{†,‡} Latifa Bouzahir-Sima,^{†,‡} Jean-Christophe Lambry,^{†,‡} Ursula Liebl,^{†,‡} Manuel Joffre,^{†,‡} and Marten H. Vos^{*,†,‡}

[†]Laboratoire d'Optique et Biosciences, Ecole Polytechnique, CNRS, and [‡]INSERM U696, 91128 Palaiseau, France

[§]Institut für Physikalische und Theoretische Chemie, Universität Würzburg, Am Hubland, 97074 Würzburg, Germany

S Supporting Information

ABSTRACT: In heme-based sensor proteins, ligand binding to heme in a sensor domain induces conformational changes that eventually lead to changes in enzymatic activity of an associated catalytic domain. The bacterial oxygen sensor FixL is the best-studied example of these proteins and displays marked differences in dynamic behavior with respect to model globin proteins. We report a mid-IR study of the configuration and ultrafast dynamics of CO in the distal heme pocket site of the sensor PAS domain FixLH, employing a recently developed method that provides a unique combination of high spectral resolution and range and high sensitivity. Anisotropy measurements indicate that CO rotates toward the heme plane upon dissociation, as is the case in globins. Remarkably, CO bound to the heme iron is tilted by $\sim 30^\circ$ with respect to the heme normal, which contrasts to the situation in myoglobin and in present FixLH–CO X-ray crystal structure models. This implies protein–environment-induced strain on the ligand, which is possibly at the origin of a very rapid docking-site population in a single conformation. Our observations likely explain the unusually low affinity of FixL for CO that is at the origin of the weak ligand discrimination between CO and O₂. Moreover, we observe orders of magnitude faster vibrational relaxation of dissociated CO in FixL than in globins, implying strong interactions of the ligand with the distal heme pocket environment. Finally, in the R220H FixLH mutant protein, where CO is H-bonded to a distal histidine, we demonstrate that the H-bond is maintained during photolysis. Comparison with extensively studied globin proteins unveils a surprisingly rich variety in both structural and dynamic properties of the interaction of a diatomic ligand with the ubiquitous *b*-type heme–proximal histidine system in different distal pockets.

Heme proteins are vital to many biological processes and fulfill versatile functions for which distinct conformational and ligand binding properties are necessary. Heme proteins that functionally interact with external diatomic ligands often contain *b*-type heme attached to the protein by a proximal histidine and possess a distal ligand-accommodation pocket. Whereas storage and transport of molecular oxygen are the most prominent functions of classical model proteins myoglobin (Mb) and hemoglobin (Hb), FixL proteins are oxygen sensors displaying very different reactivity with external ligands.¹ Here, the heme ligation state

in the PAS sensing domain, in conjunction with an attached kinase domain, can control the expression of specific microbial genes in response to changes in oxygen concentration.² Hence, substantial conformational changes upon ligand binding and release are expected to play a functional role. In recent years attempts to monitor such changes in FixL have been made on a range of time scales and with various techniques, including time-resolved X-ray crystallography.³ Additional information inferred from well-defined mutations can further help to work out analogies and contrasts between ligand dynamics in the heme pocket of FixL and globin proteins. Here we present an ultrafast study employing a recently developed chirped-pulse upconversion method^{4,5} with visible pump and mid-IR probe pulses⁶ to unveil the dynamics of photolyzed CO in the wild-type (WT) heme domain (FixLH) from *Bradyrhizobium japonicum* and the R220H mutant.

After photolysis from the heme in Mb and Hb, the CO ligand is temporarily trapped in a docking site in the distal heme pocket, as has been shown in seminal studies on Mb and Hb by Anfinrud, Lim, et al.^{7–11} Whereas heme-bound CO is oriented along the heme normal, the photolyzed CO molecules give rise to two new absorption bands corresponding to two presumably antiparallel CO orientations in which the molecular axis is nearly parallel to the heme plane.⁷ The CO molecules turn to these orientations in ~ 0.5 ps,⁹ but docking-site absorption builds up in 1.6 ps^{6,9} as a result of protein reorganization around the trapped CO. Since the CO molecules may get vibrationally excited during photolysis, a vibrational hot band that lasts for hundreds of picoseconds can also be observed,⁹ and in the case of photolysis by Soret-band excitation, CO molecules with a multiply excited vibration can be observed in the docking site.⁶

In FixL, transient resonance Raman^{12–15} and absorption spectroscopy in visible^{16–18} and mid-IR¹⁹ regions has been employed to gain insight into the dynamics after ligand photolysis. Unlike globins, virtually no heme doming occurs after O₂ photolysis,^{13,14} indications of docking-site relaxation on the nanosecond time scale exist,¹⁹ and picosecond CO geminate rebinding occurs in R220H FixLH–CO.¹⁶ In this mutant, a H-bond between heme-bound CO and the introduced distal histidine can be formed.

Our upconversion method^{4–6} allows for simultaneous measurement of the absorption of both heme-bound and docked CO with a very high density of points, high spectral resolution, and high sensitivity [see the Supporting Information (SI) for details]. This combination is particularly expedient for subtracting broad

Received: May 18, 2011

Published: October 04, 2011

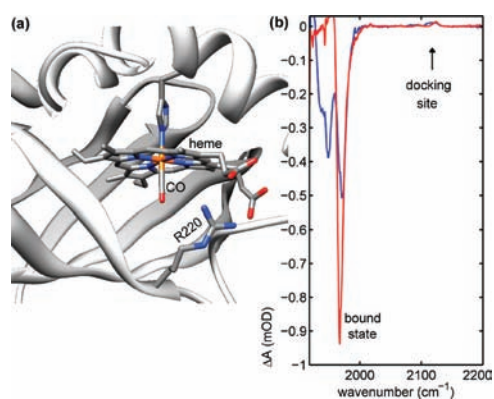


Figure 1. (a) Ribbon cartoon of the crystal structure of WT FixLH–CO (PDB entry 1XJ2). (b) Transient absorption signals of WT (red) and R220H (blue) FixLH–CO pumped at 400 nm and probed in the mid-IR after 1 ps. The pump and probe polarizations were set to the magic angle. Bound-state bleach and docking-site absorption were observed simultaneously.

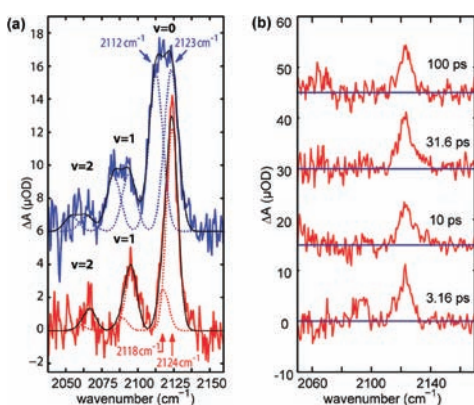


Figure 2. (a) Docking-site absorption signal of WT (red) and R220H (blue, offset by $6 \mu\text{OD}$ for clarity) FixLH–CO pumped at 400 nm and probed in the mid-IR after 1 ps (magnification of Figure 1b). The fits are shown as black solid lines, whereas each Gaussian of the fit is shown as a dotted line and labeled with its center wavenumber. The hot bands were fitted as red-shifted replicas of the dominant peak. (b) Docking-site absorption signals of WT FixLH–CO for various pump–probe delays.

heat-induced background features on which the narrow CO spectral features are superimposed.^{19,20} The high sensitivity also allows us to use a relatively optically thin sample (optical density = 0.36 at an excitation wavelength of 400 nm) under low-excitation conditions (only $\sim 3\%$ of the sample was excited), which is especially useful for interpretation of anisotropy experiments.¹⁰

After CO photolysis from the heme by Soret-band excitation with a 400 nm pump pulse, the transient absorption change of WT and R220H FixLH–CO was monitored by a mid-IR probe pulse. The bound-state bleach signal of the WT protein exhibited only one minimum (red curve in Figure 1b), but two minima were present in R220H (blue curve). The latter observation reflects the existence of an additional conformation with a H-bond between the heme-bound CO and the introduced histidine, which extends into the heme pocket.¹⁶ The H-bond effectively reduces CO bond strength, as indicated by the red-shifted peak.

Photolyzed CO is trapped in the docking site, giving rise to absorption signals around 2100 cm^{-1} . For WT, one dominant peak was observed (red line in Figure 1b, magnified in Figure 2a).

To account for the asymmetric peak shape, the peak was fitted with two Gaussians,²¹ a large one (80% amplitude) at 2124 cm^{-1} and a smaller one at 2118 cm^{-1} , resulting in a fwhm of 11 cm^{-1} for the peak (see fit in Figure 2a). The ratio of the integrated bound-state bleaching to the docking-site absorption was $\sim 55:1$.

While the high-amplitude bleaching feature of WT FixLH–CO and the presence of a dominant induced absorption band are very similar to what has been previously reported,¹⁹ we observed a different relative amplitude, maximum, and shape of the much weaker induced absorption than reported in ref 19 (high-energy shoulder at 2135 cm^{-1} , fwhm 16 cm^{-1} , relative amplitude $\sim 15:1$). These discrepancies might arise at least in part from differences in spectral resolution, recording procedure, and background subtraction. Our unique combination of high spectral resolution, density of points, and simultaneously recorded spectral range are well-suited to provide a substantial reduction in the uncertainties related to these aspects.

In our experiments, a further peak red-shifted by 29 cm^{-1} could be clearly seen in WT FixLH and the R220H mutant. In addition, for R220H FixLH–CO, there was a broader feature that, when fit by two Gaussians, comprised two curves of almost identical magnitude and a fwhm of 11 cm^{-1} with maxima at 2123 and 2112 cm^{-1} . The observation of distinct peaks in FixLH after CO photolysis can be due either to distinct docking configurations of CO (such as the two antiparallel orientations in MbCO and HbCO⁸ or the distinct states suggested for cytochrome P450²²) or to the population of different vibrational levels within the same docking site. Spectral separations of 26 cm^{-1} between two antiparallel configurations have been reported in Mb mutants.²³ Here, the peaks in WT FixLH and the R220H mutant were separated by 29 cm^{-1} and showed an identical shift in the bands; a weak third peak (again red-shifted by 29 cm^{-1}) could also be identified (Figure 2a). Therefore, we assign the observed bands to different vibrational states. We note that the vibrational energy difference of 29 cm^{-1} is higher than in gas-phase CO (26.5 cm^{-1})⁸ and the value we observed in HbCO (27.5 cm^{-1})⁶ (see below). Assuming that the three peaks all have the same shape but are replica-shifted because of anharmonicity, one finds population distributions of 85% ($\nu = 0$), 13% ($\nu = 1$), and 2% ($\nu = 2$) for WT FixLH and 84% ($\nu = 0$), 14% ($\nu = 1$), and 2% ($\nu = 2$) for R220H FixLH. These distributions are in excellent agreement with similar results for HbCO,⁶ which can be explained by the similar deposition of vibrational energy during CO photolysis with Soret excitation of the heme.

Figure 2b shows that the hot band decays within ~ 10 ps. This is in sharp contrast to the situation in HbCO, where it persists 2 orders of magnitude longer and decays only in ~ 600 ps.¹¹ The $\nu = 1 \rightarrow 0$ decay is even faster than the ~ 20 ps observed in heme-bound CO.^{24,25} The existence of the $\nu = 2$ band at a delay of 1 ps strongly argues against a fast loss of signal of a distinct orientational state, as suggested for P450,²² but corroborates the hot band assignment. We suggest that the large anharmonicity (29 cm^{-1}), reflecting a deformation of the CO potential energy surface, and the fast loss of vibrational energy originate from the same specific interactions of CO with the FixLH heme pocket. This finding further underlines the well-structured docking-site environment in HbCO and MbCO, because the CO is not only rigidly oriented (as evidenced by two narrow absorption lines) but also trapped in such a way that vibrational energy can barely be transferred away. By contrast, the less restricted orientation of CO in FixLH gives rise to a broader absorption line and more efficient disposal of the vibrational energy. Molecular dynamics simulations on CO in Mb have indicated that because of the isolated character of the CO

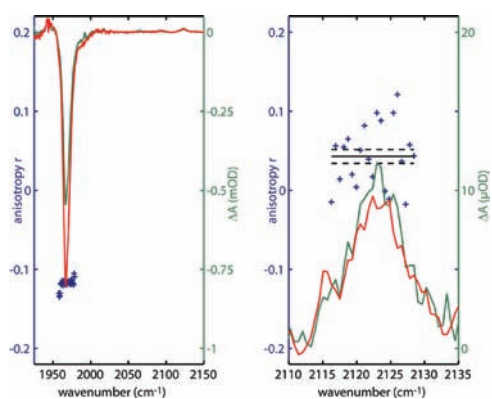


Figure 3. Transient absorption signals of a FixLH–CO sample with parallel (green) and perpendicular (red) pump and probe polarizations at a pump–probe delay of 3.2 ps. The anisotropy is shown in blue; no corrections for distortions due to a finite optical thickness have been made.¹⁰ A magnification of the $\nu = 0$ docking-site absorption signal is shown on the right. The mean anisotropy value of the central part of the peak is shown as a black solid line, and the standard errors are indicated by dashed lines.

vibration with respect to the vibrations of the surrounding atoms, the vibrational energy exchange occurs via overlap of the far tails of the involved vibrational bands, and the relaxation rate is expected to be exquisitely sensitive to the protein environment.^{11,26,27} However, such effects have not yet been experimentally explored in different heme proteins. Our present results on FixLH provide experimental support for the general notion of high sensitivity of CO vibrational energy relaxation to the protein environment.

In comparison with MbCO and HbCO,⁸ the increased width of the CO docking-site absorption in FixLH and the fact that the two distinct peaks of the globins are absent indicate that CO can adopt a range of configurations in the docking site and that the distal heme pocket is less constrained in FixLH–CO. Also, the asymmetric peak shape most likely is not due to distinct CO orientations but rather to a distribution of CO configurations, as was also argued for a modified cytochrome *c*.²¹

With regard to the onset of the docking-site signal, our data are in agreement with previous observations,¹⁹ where maximum docking-site absorption was found after photolysis and a slight decrease in the signal within 6 ps was deduced. This is in further clear contrast to HbCO and MbCO, which exhibit a rise time of 1.6 ps^{6,9} needed for protein rearrangement around the well-oriented, trapped CO molecules. To determine whether this more rapid appearance of the maximum docking-site absorption for FixLH–CO might originate from a difference in the extent of CO reorientation in the heme pocket upon dissociation, we performed anisotropy measurements (Figure 3). In the limit of homogeneous and nonsaturating excitation, the anisotropy r of a linear absorber (CO) after excitation of a circular absorber (heme) is related to the angle θ between the direction of the CO transition dipole moment and the heme normal as $r = (3\langle \sin^2 \theta \rangle - 2)/10$.^{10,28} If the docked CO is oriented randomly, the docking site would have $r = 0$, whereas r could be as large as 0.1 if the CO is oriented perpendicular to the normal of the heme. We found an average r value ~ 0.04 (corresponding to an average angle $\theta \sim 64^\circ$), similar to the average values observed for Hb and Mb.⁷ This suggests that CO in the FixL docking site is also oriented at a large angle with respect to the heme normal. In contrast to globins, within the noise no variation of r over the band was observed, indicating that no distinct docking configurations are occupied. Together, these

experiments point to the occupation of a single CO orientation in the docking site, although the presence of two antiparallel configurations with identical spectral properties, such as proposed for the Mb H64L mutant,²³ cannot be excluded.

Whereas the anisotropy of bleaching of the CO-bound form measured for HbCO under the same conditions was close to -0.2 (see Figure S1 in the SI), in full agreement with previous measurements¹⁰ and implying a nearly perpendicular CO configuration, it had a substantially higher value ($r \approx -0.12$) in FixLH. This indicates that the bound CO makes a substantial angle with the heme normal ($\theta_{\text{avg}} \approx 30^\circ$). We note that the heme may deviate from a pure circular absorber at 400 nm, although such deviations appear to be small for Soret absorptions of globins.²⁹ Nevertheless, even for the (unlikely) extreme case of a linear absorber, our observed r value of -0.12 corresponds to $\theta \approx 21^\circ$. The corresponding angles in two different X-ray structural models vary from 16° in PDB entry 1LSV³⁰ to 8° in PDB entry 1XJ2,³¹ which are significantly lower than the value we observed. The Fe–C–O angle (note that the Fe–C axis is not necessarily strictly along the heme normal) derived from EXAFS measurements of FixL from *Rhizobium meliloti* in solution was 157° ,³² and a comparative resonance Raman analysis indicated that this angle is even smaller in FixLH from *B. japonicum*.³³ Our results suggest either the CO configuration is perturbed in various ways in crystals with respect to solution or the difference is within the resolution of the structures. Crystallography with crystals diffracting to atomic resolution³⁴ might provide additional insight but is presently not available for FixLH. Our studies imply that in contrast to Mb and Hb, the protein environment in oxygen sensor FixL does impose strain on bound CO, causing it to tilt away from the perpendicular orientation found in heme–CO complexes in solution. To our knowledge, since the spectroscopic demonstration of nearly perpendicular CO–heme orientation in MbCO by Anfinsen et al.⁷ no other counterexamples of protein-induced CO bending like that observed here for FixLH have been documented.

The detailed structural origin of the CO tilt remains to be determined but possibly involves Ile residues 215 and 238 in the distal heme pocket, which are in close interaction with CO and change configuration in different ligation states.³⁰ As an important functional consequence, our findings can explain the unusually low CO affinity of FixL (~ 300 times lower than that of Mb) that is at the origin of the very weak ligand discrimination between CO and O₂ in this oxygen sensor protein.¹

X-ray diffraction studies indicate that CO binding does not induce a change in the protein backbone of crystalline FixLH toward the signaling O₂-bound form.³⁰ Nevertheless, CO does inhibit, albeit modestly, kinase activity in FixL.³⁵ The difference between our findings of CO orientation in FixLH in solution and those in crystals may indicate that structural changes transmitted to the kinase domain are actually induced by CO, possibly explaining this discrepancy.

The combined orientation results of the bound and dissociated states indicate that the orientation change with respect to the heme normal is substantially less in FixL than in globins. We suggest that the presence of a bent CO-bound state can explain the faster population of the docking site and the apparent absence of distinct antiparallel docking-site orientations.

For the R220H mutant protein, the H-bond between CO and the distal histidine present in part of the population leads to an additional red-shifted peak for heme-bound CO that is observable in the bound-state bleach (blue line in Figure 1b). It also leads to an additional red-shifted absorption for the docked CO (Figure 2a),

strongly suggesting that upon photolysis the Fe–CO bond is broken, but not the H-bond: if the CO were able to turn into the antiparallel orientation, a band should appear at higher frequencies. One could argue that the H-bond might also be broken but immediately reformed by a fraction of the photolyzed CO molecules. If this were the case, then the red-shifted peak of the bound-state bleach and the red-shifted peak of the docking-site absorption would not be directly connected. For a Mb mutant, Hamm et al.³⁶ showed by two-dimensional IR spectroscopy that this connection indeed exists. We conjecture that the same applies to the FixLH mutant; 2DIR experiments could provide direct evidence.

In R220H FixL–CO, substantial partial geminate rebinding of photolyzed CO (with a 250 ps time constant) was demonstrated by transient absorption spectroscopy in the visible spectral regime,¹⁶ and pH-dependence studies indicated that the fraction carrying a H-bond between CO and the introduced histidine is responsible for it.¹⁶ If proteins in which CO is H-bonded maintain the H-bond on the time scale of rebinding, only the red-shifted features would be expected to show a 250 ps decay component. In our data (Figure S2), the ratio of photolyzed CO with and without the H-bond did not change as a function of time; instead, the overall signal (e.g., both minima in the bound-state bleach) decreased. This suggests that conformational switching (i.e., cleavage and formation of H-bonds with distal histidine) occurs on a time scale shorter than 250 ps. This finding is in general agreement with 2DIR experiments by Fayer et al.³⁷ showing that in a Mb mutant, such conformational switching proceeds on a time scale of several tens of picoseconds. The ensemble of data indicates that H-bonding equilibria between CO and distal histidine are established on the picosecond time scale but not directly perturbed by rupture of the heme–CO bond.

In summary, we have shown that the primary CO ligand dynamics in ligand-sensor FixL proteins is distinctly different from that in ligand-carrier globin proteins. The CO ligand, bound in a remarkable protein-induced bent configuration, can upon dissociation be rapidly trapped in a single, less structured docking site in which the ligand's vibrational energy can be disposed readily and its configuration is less restricted. In perspective, understanding of the surprisingly rich variety in both structural and dynamic properties of the interaction of a diatomic ligand with the ubiquitous *b*-type heme–proximal histidine system in different distal pockets unveiled in our spectroscopic work will provide a challenge requiring detailed structural and modeling studies.

■ ASSOCIATED CONTENT

S Supporting Information. Materials and methods, anisotropy of HbCO, and details of the bound-state bleach signal of R220H FixLH–CO. This material is available free of charge via the Internet at <http://pubs.acs.org>.

■ AUTHOR INFORMATION

Corresponding Author
marten.vos@polytechnique.edu

■ ACKNOWLEDGMENT

This work was supported by the Agence Nationale de la Recherche (ANR-06-BLAN-0286). P.N. acknowledges financial support from the Deutsche Akademie der Naturforscher Leopoldina (BMBF-LPDS 2009-6).

■ REFERENCES

- (1) Gilles-Gonzalez, M. A.; Gonzalez, G.; Perutz, M. F.; Kiger, L.; Marden, M. C.; Poyart, C. *Biochemistry* **1994**, *33*, 8067.
- (2) Gilles-Gonzalez, M. A.; Ditta, G. S.; Helinski, D. R. *Nature* **1991**, *350*, 170.
- (3) Key, J.; Srajer, V.; Pahl, R.; Moffat, K. *Biochemistry* **2007**, *46*, 4706.
- (4) Kubarych, K. J.; Joffre, M.; Moore, A.; Belabas, N.; Jonas, D. M. *Opt. Lett.* **2005**, *30*, 1228.
- (5) Lee, K. F.; Nuernberger, P.; Bonvalet, A.; Joffre, M. *Opt. Express* **2009**, *17*, 18738.
- (6) Nuernberger, P.; Lee, K. F.; Bonvalet, A.; Vos, M. H.; Joffre, M. *J. Phys. Chem. Lett.* **2010**, *1*, 2077.
- (7) Lim, M.; Jackson, T. A.; Anfinrud, P. A. *Science* **1995**, *269*, 962.
- (8) Lim, M.; Jackson, T. A.; Anfinrud, P. A. *J. Chem. Phys.* **1995**, *102*, 4355.
- (9) Lim, M.; Jackson, T. A.; Anfinrud, P. A. *Nat. Struct. Biol.* **1997**, *4*, 209.
- (10) Lim, M.; Jackson, T. A.; Anfinrud, P. A. *J. Am. Chem. Soc.* **2004**, *126*, 7946.
- (11) Sagnella, D. E.; Straub, J. E.; Jackson, T. A.; Lim, M.; Anfinrud, P. A. *Proc. Natl. Acad. Sci. U.S.A.* **1999**, *96*, 14324.
- (12) Hiruma, Y.; Kikuchi, A.; Tanaka, A.; Shiro, Y.; Mizutani, Y. *Biochemistry* **2007**, *46*, 6086.
- (13) Kruglik, S. G.; Jasaitis, A.; Hola, K.; Yamashita, T.; Liebl, U.; Martin, J.-L.; Vos, M. H. *Proc. Natl. Acad. Sci. U.S.A.* **2007**, *104*, 7408.
- (14) Kruglik, S. G.; Lambry, J.-C.; Martin, J.-L.; Vos, M. H.; Négrerie, M. *J. Raman Spectrosc.* **2011**, *42*, 265.
- (15) Rodgers, K. R.; Lukat-Rodgers, G. S.; Tang, L. *J. Am. Chem. Soc.* **1999**, *121*, 11241.
- (16) Jasaitis, A.; Hola, K.; Bouzhir-Sima, L.; Lambry, J.-C.; Balland, V.; Vos, M. H.; Liebl, U. *Biochemistry* **2006**, *45*, 6018.
- (17) Liebl, U.; Bouzhir-Sima, L.; Négrerie, M.; Martin, J.-L.; Vos, M. H. *Proc. Natl. Acad. Sci. U.S.A.* **2002**, *99*, 12771.
- (18) Miksovská, J.; Suquet, C.; Satterlee, J. D.; Larsen, R. W. *Biochemistry* **2005**, *44*, 10028.
- (19) van Wilderen, L. J. G. W.; Key, J. M.; Van Stokkum, I. H. M.; van Grondelle, R.; Groot, M. L. *J. Phys. Chem. B* **2009**, *113*, 3292.
- (20) Lian, T.; Locke, B.; Kholodenko, Y.; Hochstrasser, R. M. *J. Phys. Chem.* **1994**, *98*, 11648.
- (21) Kim, J.; Park, J.; Lee, T.; Lim, M. *J. Phys. Chem. B* **2009**, *113*, 260.
- (22) Rupenyán, A.; Commandeur, J.; Groot, M. L. *Biochemistry* **2009**, *48*, 6104.
- (23) Nienhaus, K.; Olson, J. S.; Franzen, S.; Nienhaus, G. U. *J. Am. Chem. Soc.* **2005**, *127*, 40.
- (24) Owrutsky, J. C.; Li, M.; Locke, B.; Hochstrasser, R. M. *J. Phys. Chem.* **1995**, *99*, 4842.
- (25) Ventalon, C.; Fraser, J. M.; Vos, M. H.; Alexandrou, A.; Martin, J.-L.; Joffre, M. *Proc. Natl. Acad. Sci. U.S.A.* **2004**, *101*, 13216.
- (26) Devereux, M.; Meuwly, M. *J. Phys. Chem. B* **2009**, *113*, 13061.
- (27) Skinner, J. L.; Park, K. *J. Phys. Chem. B* **2001**, *105*, 6716.
- (28) Moore, J. N.; Hansen, P. A.; Hochstrasser, R. M. *Proc. Natl. Acad. Sci. U.S.A.* **1988**, *85*, 5062.
- (29) Eaton, W. A.; Hofrichter, J. *Methods Enzymol.* **1981**, *76*, 175.
- (30) Hao, B.; Isaza, C.; Arndt, J.; Soltis, M.; Chan, M. K. *Biochemistry* **2002**, *41*, 12952.
- (31) Key, J.; Moffat, K. *Biochemistry* **2005**, *44*, 4627.
- (32) Miyatake, H.; Mukai, M.; Adachi, S.-i.; Nakamura, H.; Tamura, K.; Iizuka, T.; Shiro, Y.; Strange, R. W.; Hasnain, S. S. *J. Biol. Chem.* **1999**, *274*, 23176.
- (33) Tomita, T.; Gonzalez, G.; Chang, A. L.; Ikeda-Saito, M.; Gilles-Gonzalez, M. A. *Biochemistry* **2002**, *41*, 4819.
- (34) Kachalova, G. S.; Popov, A. N.; Bartunik, H. D. *Science* **1999**, *284*, 473.
- (35) Dunham, C. M.; Dioum, E. M.; Tuckerman, J. R.; Gonzalez, G.; Scott, W. G.; Gilles-Gonzalez, M.-A. *Biochemistry* **2003**, *42*, 7701.
- (36) Bredenbeck, J.; Helbing, J.; Nienhaus, K.; Nienhaus, G. U.; Hamm, P. *Proc. Natl. Acad. Sci. U.S.A.* **2007**, *104*, 14243.
- (37) Ishikawa, H.; Kwak, K.; Chung, J. K.; Kim, S.; Fayer, M. D. *Proc. Natl. Acad. Sci. U.S.A.* **2008**, *105*, 8619.